Advances in sampling methods for inverse scattering problems

Dinh-Liem Nguyen

Kansas State University

Conference on Analysis and Applied Mathematics - 2020
Faculty of Mathematics and Applications
Saigon University

Funding from NSF (DMS-1812693) is gratefully acknowledged

Outline

1. Introduction
   - Inverse scattering: motivations and challenges
   - Why sampling methods?
2. An inverse medium scattering problem
   - Sampling method
   - Numerical study for simulated and experimental data
3. Locating and quantifying point scatterers
   - Sampling method
   - Numerical simulations

Direct and inverse scattering

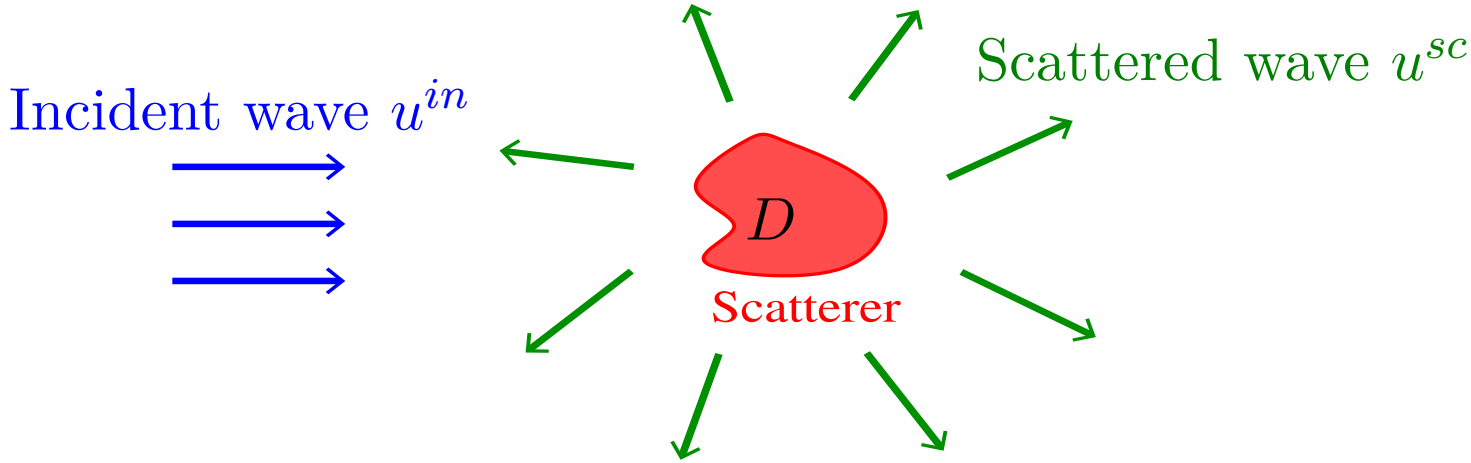

$$\begin{cases} u \text{ is governed by partial differential equation} \\ u = u^{in} + u^{sc} \quad \text{(total wave)} \\ u^{sc} \text{ is outgoing wave} \quad \text{(radiation condition)} \end{cases}$$

Direct and inverse scattering

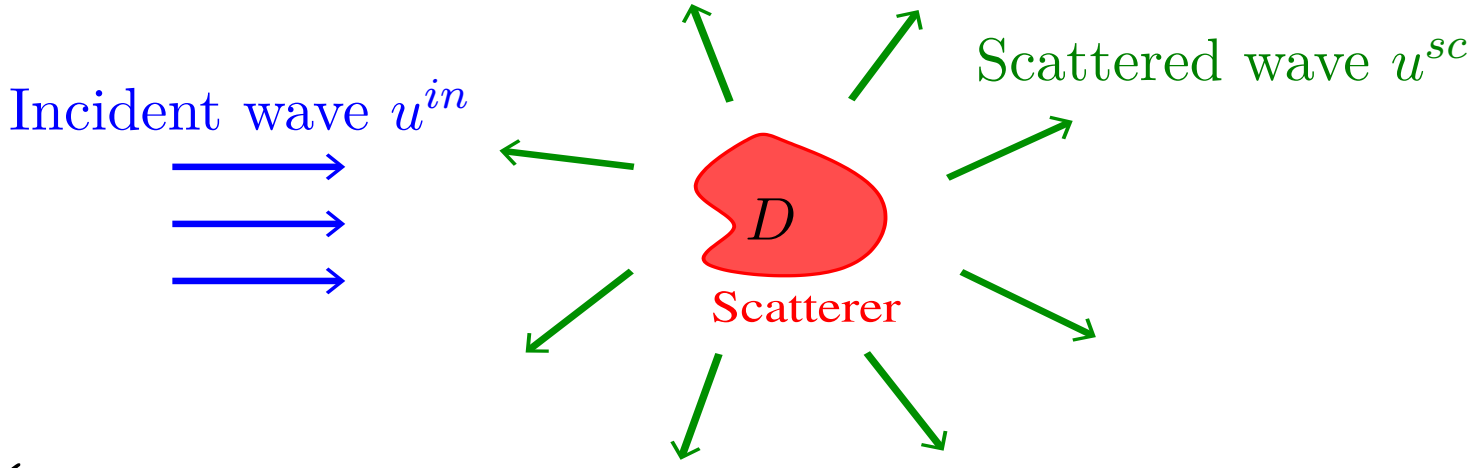

$$\begin{cases} u \text{ is governed by partial differential equation} \\ u = u^{in} + u^{sc} \quad \text{(total wave)} \\ u^{sc} \text{ is outgoing wave} \quad \text{(radiation condition)} \end{cases}$$

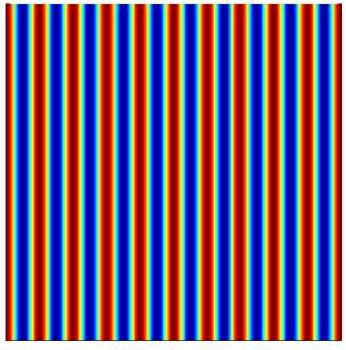

$u^{in} = e^{i10x}$

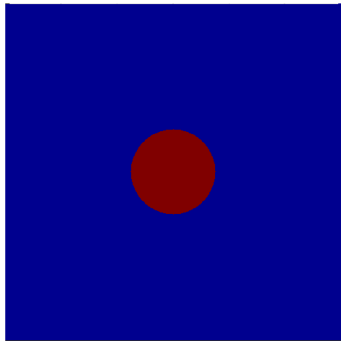

scatterer

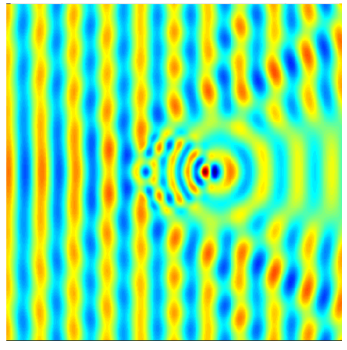

u

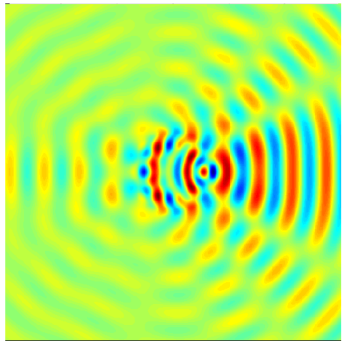

u^{sc}

Direct and inverse scattering

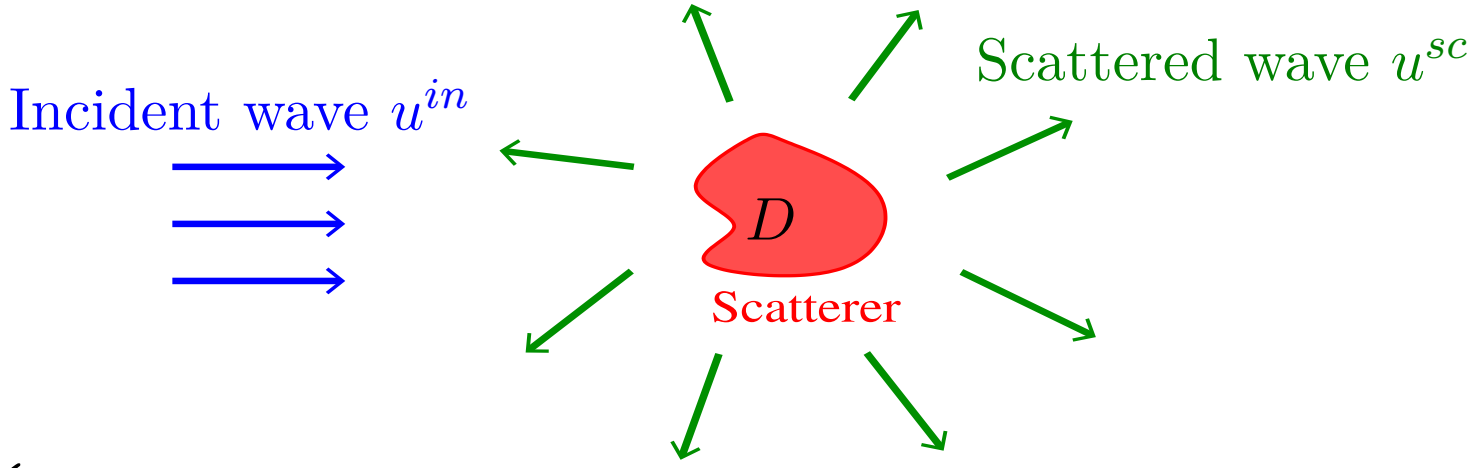

$$\begin{cases} u \text{ is governed by partial differential equation} \\ u = u^{in} + u^{sc} \quad \text{(total wave)} \\ u^{sc} \text{ is outgoing wave} \quad \text{(radiation condition)} \end{cases}$$

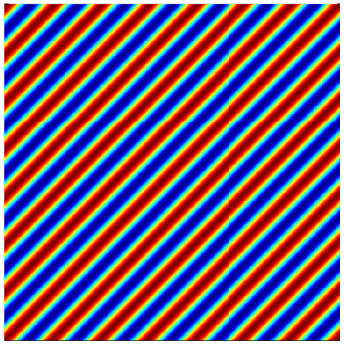

u^{in}

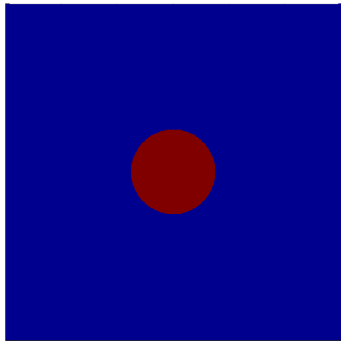

scatterer

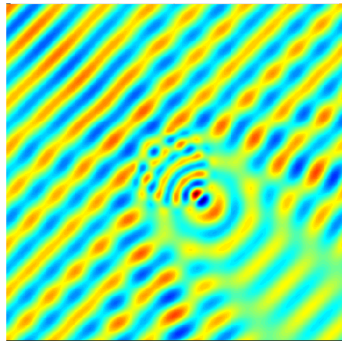

u

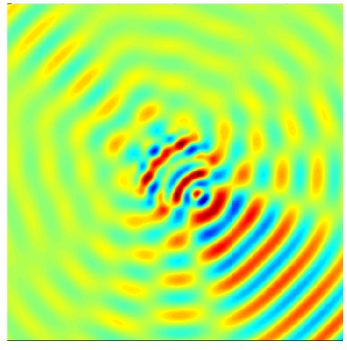

u^{sc}

Direct and inverse scattering

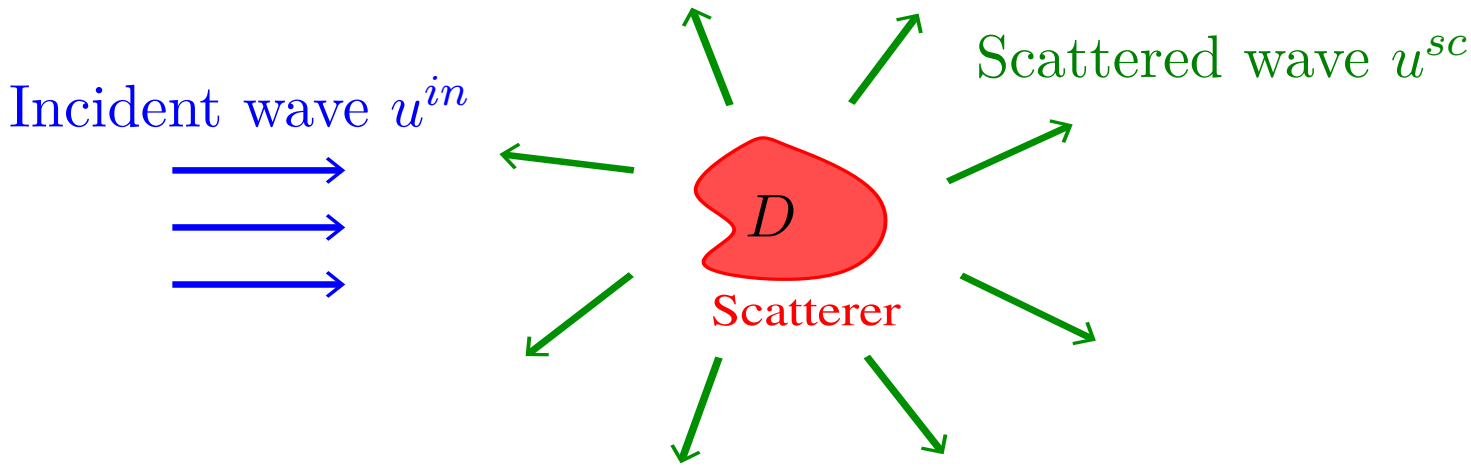

Direct problem: Determine scattered wave u^{sc} from knowledge of incident wave u^{in} and the scatterer.

Inverse problem: Determine the scatterer from boundary measurements of scattered wave u^{sc} (for several incident waves u^{in}).

Inverse scattering: motivations & challenges

- Applications: non-destructive evaluation, detection of explosives, geophysical exploration, medical imaging, radar, material characterization ...

(a) Non-destructive testing

(b) Detection of explosives

Inverse scattering: motivations & challenges

- Applications: non-destructive testing, detection of explosives, geophysical exploration, medical imaging, radar, material characterization ...

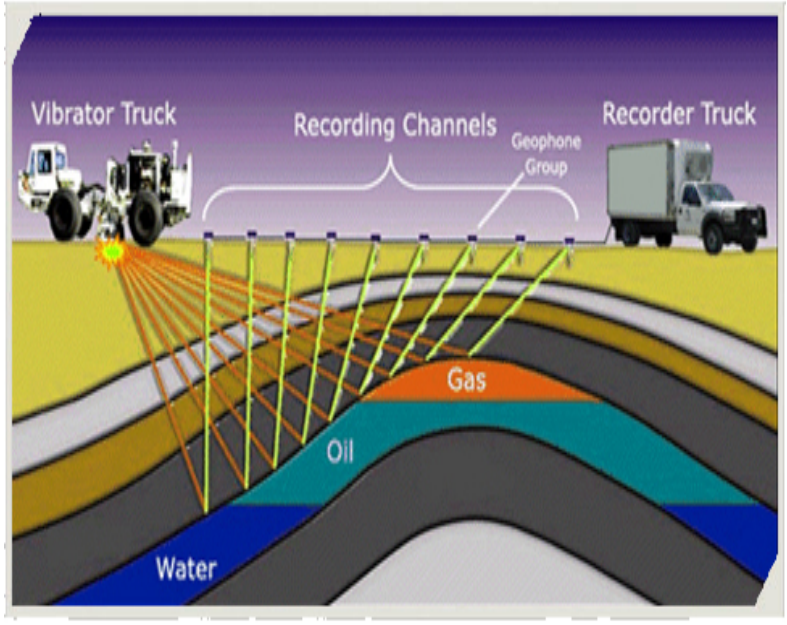

(c) Geophysical exploration

(d) Medical imaging

Inverse scattering: motivations & challenges

- Inverse problems in the language of partial differential equations (PDEs): Recover a coefficient (or its domain of definition) of a PDE from boundary measurements of its solution.

Inverse scattering: motivations & challenges

- Inverse problems in the language of partial differential equations (PDEs): Recover a coefficient (or its domain of definition) of a PDE from boundary measurements of its solution.
- **Major challenges:**
  - nonlinear problems
    Example: $u'(t) = au(t)$, $u(0) = 1$ ($a = constant$).

    Inverse problem of finding a from $u(t)$ is nonlinear ($u(t) = e^{at}$ depends nonlinearly on coefficient a.)

Inverse scattering: motivations & challenges

- Inverse problems in the language of partial differential equations (PDEs): Recover a coefficient (or its domain of definition) of a PDE from boundary measurements of its solution.
- **Major challenges:**
  - nonlinear problems
    Example: $u'(t) = au(t)$, $u(0) = 1$ ($a = constant$).
    Inverse problem of finding a from $u(t)$ is nonlinear ($u(t) = e^{at}$ depends nonlinearly on coefficient a.)
  - unstable with respect to measurement error (ill-posed problems)
    Example: $u''(t) = q(t)$, $u(0) = u'(0) = 0$.
    Assume $u_{measured}(t) = u(t) + \frac{1}{10^9}\cos(10^9 t)$ (small error).
    Then $q_{approx}(t) = q(t) - 10^9 \cos(10^9 t)$ (large error).
    Inverse problem of finding q_{approx} from $u_{measured}$ is unstable.
  - uniqueness is not guaranteed with only several measurements?

Inverse scattering: motivations & challenges

- There is a vast literature on studies of uniqueness and stability of inverse problems.
  Monographs:
  - D. Colton & R. Kress, *Inverse acoustic and electromagnetic scattering theory* (Springer, 3rd edition 2013).
  - V. Isakov, *Inverse problems for partial differential equations* (Springer, 3rd edition 2017).
  - A. Kirsch, *An introduction to the mathematical theory of inverse problems* (Springer, 2nd edition 2011).

- Numerical reconstruction methods aim to find approximate solution of inverse problems.

Optimization for inverse scattering

- Recall D in the scatterer and $u^{\text{sc}}|_\Gamma$ as boundary values of the scattered field.
- Consider mapping $F(D) = u^{\text{sc}}|_\Gamma$, data $= u^{\text{sc}}|_\Gamma$ + noise
- The most studied approach for inverse scattering problems is optimization-based methods:

$$\min_D \|F(D) - \text{data}\|.$$

  - Advantages: accurate (when they converge!), applicable to coefficient reconstructions.
  - Limitations: computationally expensive, local minima, require detailed *a priori* information of the solution (e.g. number of connected components, types of boundary conditions are known in advance.)

- Sampling methods can avoid these limitations!

What are sampling methods?

Sampling: Suppose the scatterer is searched in larger domain Ω. We discretize Ω using a set of sampling points z.

Goal: Construct an (approximate) indicator function $I(z)$ for the scatterer (i.e. $I(z) \approx 1$ inside scatterer, $I(z) \approx 0$ outside scatterer).

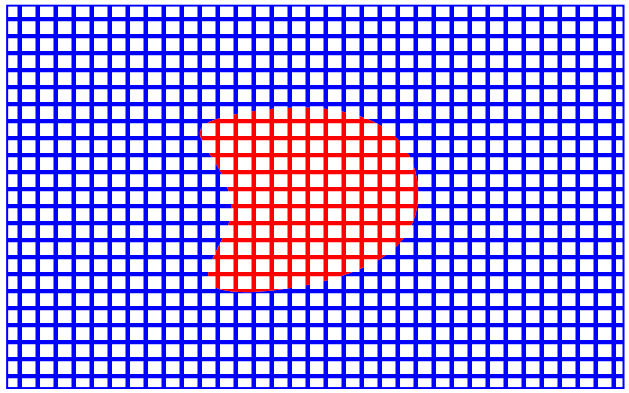

- Advantages: Construction of $I(z)$ from the data essentially does not require *a priori* information about the scatterer, and its computation is simple, fast, and non-iterative.
- Limitations: Some sampling methods use more data than optimization, not applicable to coefficient reconstructions.

What are sampling methods?

- Linear sampling method, Colton & Kirsch 1996
- Point source method, Potthast 1996
- Factorization method, Kirsch 1998
- Probe method, Ikehata 1998
- Singular sources method, Potthast 1999
- Enclosure method, Ikehata 1999
- Range test method, Potthast, Sylvester & Kusiak 2003
- Reciprocity gap functional method, Colton & Haddar 2005
- Orthogonality sampling method, Potthast 2010
- Direct sampling method, Ito, Jin & Zou 2012
- Generalized linear sampling method, Audibert & Haddar 2014

  ...

Reference books for classical sampling methods

- Cakoni & Colton (2006) Qualitative Methods in Inverse Scattering Theory
- Kirsch & Grinberg (2008) The Factorization Method for Inverse Problems

Orthogonality sampling method

Orthogonality sampling method for far-field measurement

- Helmholtz equation: **Potthast 2010** (one-wave data), Griesmaier 2011 (multi-frequency data), Liu 2017 (multi-wave data)
- Maxwell's equations: N. 2019 (one-wave data), Harris & N. 2020 (multi-wave data)

Compare with classical sampling methods:

- Simpler implementation (no regularization needed)
- Stability justified
- Versatility (one-wave/multi-wave/multi-frequency data)

This talk: A sampling method sharing these advantages and work for measurements at any distance and for other applications.

Outline

1. Introduction
   - Inverse scattering: motivations and challenges
   - Why global reconstruction methods?
2. An inverse medium scattering problem
   - Sampling method
   - Numerical study for simulated and experimental data
3. Locating and quantifying point scatterers
   - Sampling method
   - Numerical simulations

Inverse scattering problem with Cauchy data

- Let $\eta : \mathbb{R}^2 \to \mathbb{C}$ be bounded function satisfying $\eta = 0$ in $\mathbb{R}^n \setminus \overline{D}$. Let Ω be a domain such that $D \subset \Omega$. Consider incident waves $u^{in}(x, d) = e^{ik\theta \cdot x}$, $\theta \in S := \{x \in \mathbb{R}^2 : |x| = 1\}$

- Consider the following model problem

$$\begin{cases} \Delta u + k^2(1 + \eta(x))u = 0 \quad \text{in } \mathbb{R}^2 \\ u = u^{in} + u^{sc} \\ \lim\limits_{|x|\to\infty} |x| \left(\frac{x}{|x|} \cdot \nabla u^{sc} - iku^{sc} \right) = 0. \end{cases}$$

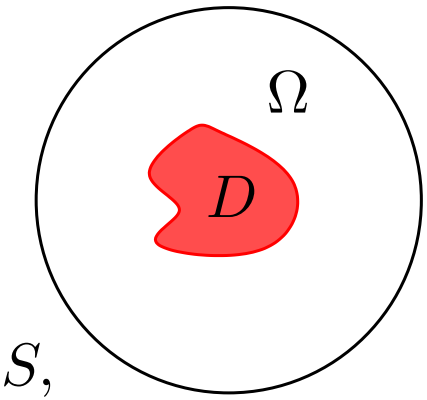

- **Inverse Problem: Given**

$$u^{sc}(\cdot, \theta)|_{\partial\Omega}, \quad \partial_\nu u^{sc}(\cdot, \theta)|_{\partial\Omega}, \quad \forall \theta \in S,$$

determine D (shape and location).

A sampling method

We define the imaging functional as

$$I(z) := \int_S \left| \int_{\partial\Omega} \left(\frac{\partial \mathrm{Im}\, \Phi(x,z)}{\partial \nu(x)} u^{sc}(x,\theta) - \mathrm{Im}\, \Phi(x,z) \frac{\partial u^{sc}(x,\theta)}{\partial \nu(x)} \right) ds(x) \right|^2 ds(\theta),$$

where $\Phi(x,z)$ is the Green's function of the direct problem ($\Phi(x,z) = H_0^{(1)}(k|x-z|)$, Hankel function of first kind and zero order).

Claims:

- $I(z)$ will take large values inside scatterer D and small values outside D.

A sampling method

We define the imaging functional as

$$I(z) := \int_S \left| \int_{\partial\Omega} \left(\frac{\partial \mathrm{Im}\, \Phi(x,z)}{\partial \nu(x)} u^{sc}(x,\theta) - \mathrm{Im}\, \Phi(x,z) \frac{\partial u^{sc}(x,\theta)}{\partial \nu(x)} \right) ds(x) \right|^2 ds(\theta),$$

where $\Phi(x,z)$ is the Green's function of the direct problem ($\Phi(x,z) = H_0^{(1)}(k|x-z|)$, Hankel function of first kind and zero order).

Claims:

- $I(z)$ will take large values inside scatterer D and small values outside D.
- Plotting $I(z)$ for many sampling points z will give us an (approximate) image of the scatterer D.

A sampling method

We define the imaging functional as

$$I(z) := \int_S \left| \int_{\partial\Omega} \left(\frac{\partial \mathrm{Im}\, \Phi(x,z)}{\partial \nu(x)} u^{sc}(x,\theta) - \mathrm{Im}\, \Phi(x,z) \frac{\partial u^{sc}(x,\theta)}{\partial \nu(x)} \right) ds(x) \right|^2 ds(\theta),$$

where $\Phi(x,z)$ is the Green's function of the direct problem ($\Phi(x,z) = H_0^{(1)}(k|x-z|)$, Hankel function of first kind and zero order).

Claims:

- $I(z)$ will take large values inside scatterer D and small values outside D.
- Plotting $I(z)$ for many sampling points z will give us an (approximate) image of the scatterer D.

WHY?

Far-field operator and its factorization

- For all $(\hat{x}, \theta) \in S \times S$,

$$u^{sc}(x, \theta) = \frac{e^{ik|x|}}{|x|^{1/2}}(u^{\infty}(\hat{x}, \theta) + O(1/|x|)), \quad |x| \to \infty,$$

  where $u^{\infty}(\hat{x}, \theta)$ is called the far-field pattern.
- Define far-field operator $F : L^2(S) \to L^2(S)$ as

$$Fg(\hat{x}) = \int_S u^{\infty}(\hat{x}, \theta) g(\theta) ds(\theta).$$

- Define solution operator $G : L^2(D) \to L^2(S)$ as

$$Gf = w^{\infty},$$

  where w^{∞} is the far-field pattern of unique solution w to the direct problem with $u^{in} = f$.

Far-field operator and its factorization

- For all $(\hat{x}, \theta) \in S \times S$,

$$u^{sc}(x, \theta) = \frac{e^{ik|x|}}{|x|^{1/2}}(u^{\infty}(\hat{x}, \theta) + O(1/|x|)), \quad |x| \to \infty,$$

  where $u^{\infty}(\hat{x}, \theta)$ is called the far-field pattern.
- Define far-field operator $F : L^2(S) \to L^2(S)$ as

$$Fg(\hat{x}) = \int_S u^{\infty}(\hat{x}, \theta) g(\theta) ds(\theta).$$

- Define solution operator $G : L^2(D) \to L^2(S)$ as

$$Gf = w^{\infty},$$

  where w^{∞} is the far-field pattern of unique solution w to the direct problem with $u^{in} = f$.
- We have

$$Fg = G\left[\int_S u^{in}(x, \theta) g(\theta) ds(\theta)\right].$$

Far-field operator and its factorization

- Recall $u^{in}(x,\theta) = e^{ik\theta\cdot x}$, $Fg = G\left[\int_S u^{in}(x,\theta)g(\theta)ds(\theta)\right]$.
- Define Herglotz operator $H : L^2(S) \to L^2(D)$ as

$$Hg(x) = \int_S e^{ik\theta\cdot x} g(\theta) ds(\theta).$$

- Then $F = GH$.
- **Lemma.**

$$F = H^* T H$$

where $T : L^2(D) \to L^2(D)$ is given by

$$Tf = k^2\eta(f + w),$$

where w solves the direct problem with $u^{in} = f$.

Far-field operator and its factorization

- Recall $F = H^* T H$
- **Assumption 1.** Assume that $\eta \in L^\infty(\mathbb{R}^2)$, $\mathrm{Im}\,(\eta) \geq 0$ and that there exists constant $c > 0$ such that $\mathrm{Re}\,(\eta(x)) + \mathrm{Im}\,(\eta(x)) \geq c$ for almost all $x \in D$.
- **Theorem.** a) Let

$$\phi_z(\theta) = e^{-ikz\cdot\theta}, \quad z \in \mathbb{R}^2, \quad \theta \in S \tag{1}$$

Then $\phi_z \in \mathrm{Range}(H^*)$ if and only if $z \in D$.
b) If k is not an interior transmission eigenvalue and Assumption 1 holds true, then there exists constant $C > 0$ such that

$$|\langle Tf, f\rangle| \geq C\|f\|^2, \quad \text{for all } f \in \mathrm{Range}(H).$$

Far-field operator and its factorization

Recall

$$I(z) = \int_S \left| \int_{\partial\Omega} \left(\frac{\partial \mathrm{Im}\, \Phi(x,z)}{\partial \nu(x)} u^{sc}(x,\theta) - \mathrm{Im}\, \Phi(x,z) \frac{\partial u^{sc}(x,\theta)}{\partial \nu(x)} \right) ds(x) \right|^2 ds(\theta).$$

- **Lemma.** (N. 2020)

$$I(z) = c \|F\phi_z\|^2$$

where c is a positive constant and

$$\phi_z(\theta) = e^{-ikz\cdot\theta}, \quad z \in \mathbb{R}^2, \quad \theta \in S.$$

Key ingredients of proof:
Using the Funk-Hecke formula to show that Herglotz operator $H\varphi_z$ is proportional to $\mathrm{Im}\, \Phi(\cdot, z)$
Reciprocity relation $u^\infty(\hat{x}, \theta) = u^\infty(-\theta, -\hat{x})$

Far-field operator and its factorization

Recall

$$I(z) = \int_S \left| \int_{\partial\Omega} \left(\frac{\partial \mathrm{Im}\, \Phi(x,z)}{\partial \nu(x)} u^{sc}(x,\theta) - \mathrm{Im}\, \Phi(x,z) \frac{\partial u^{sc}(x,\theta)}{\partial \nu(x)} \right) ds(x) \right|^2 ds(\theta).$$

- **Theorem 1.** (N. 2020) For $z \in D$ there exists constant $\gamma_z > 0$ such that

$$I(z) \geq \gamma_z.$$

Key ingredients of proof:

$$\begin{aligned} I(z) = c_1 \|F\phi_z\|^2 &\geq c_2 |\langle F\phi_z, \phi_z \rangle|^2 \\ &= c_2 |\langle H^* T H \phi_z, \phi_z \rangle|^2 \\ &= c_2 |\langle T H \phi_z, H \phi_z \rangle|^2 \\ &\geq c_3 \|H\phi_z\|^4 \quad (T \text{ is coercive}). \end{aligned}$$

Then use the lemma for characterization of D to derive the desired estimate.

Far-field operator and its factorization

- **Theorem 2.** (N. 2020) The imaging functional $I(z)$ satisfies

$$I(z) = \int_S \left| k^2 \int_D J_0(k|z-y|)\eta(y)u(y,\theta)dy \right|^2 ds(\theta).$$

  where J_0 is the Bessel function of the first kind.

- **Corollary.**

$$I(z) = O\left(\frac{1}{\text{dist}(z, D)}\right).$$

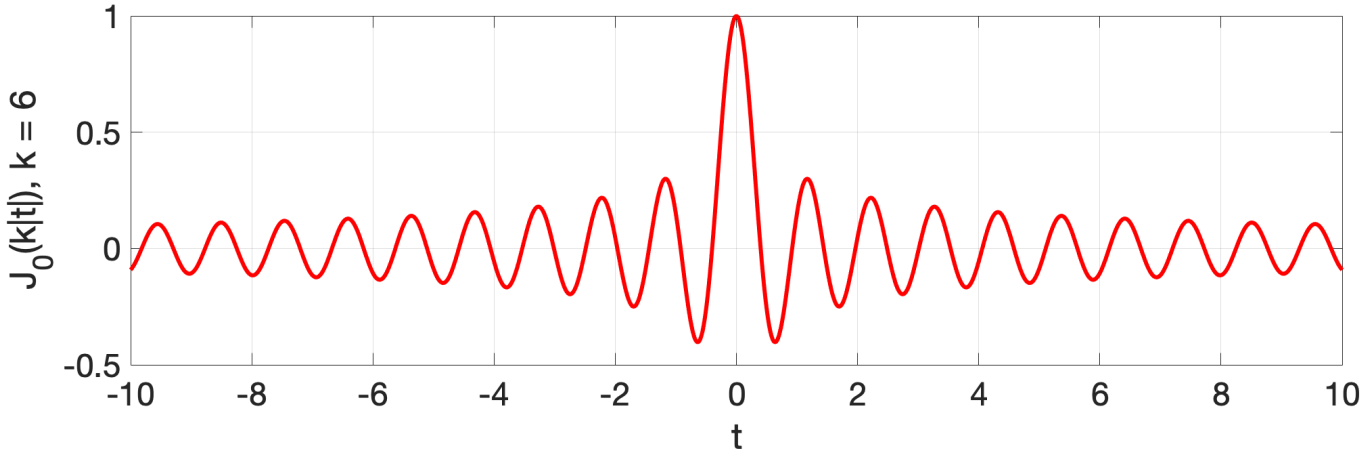

Stability against noise

We assume the noisy data u_{sc}^{δ} and $\partial u_{\mathrm{sc}}^{\delta}/\partial\nu$ satisfy

$$\|u_{\mathrm{sc}} - u_{\mathrm{sc}}^{\delta}\|_{L^2(\partial\Omega\times S)} \leq \delta_1 \|u_{\mathrm{sc}}\|_{L^2(\partial\Omega\times S)},$$
$$\left\| \frac{\partial u_{\mathrm{sc}}}{\partial\nu} - \frac{\partial u_{\mathrm{sc}}^{\delta}}{\partial\nu} \right\|_{L^2(\partial\Omega\times S)} \leq \delta_2 \left\| \frac{\partial u_{\mathrm{sc}}}{\partial\nu} \right\|_{L^2(\partial\Omega\times S)},$$

for some positive constants δ_1, δ_2.

Theorem 3. (N. 2020) Let $I^{\delta}(z)$ the imaging functional with noisy data u_{sc}^{δ} and $\partial u_{\mathrm{sc}}^{\delta}/\partial\nu$. Then

$$I(z) - I^{\delta}(z) \leq C \min(\delta_1^2, \delta_2^2), \quad \text{for all } z \in \mathbb{R}^2.$$

Numerical simulations

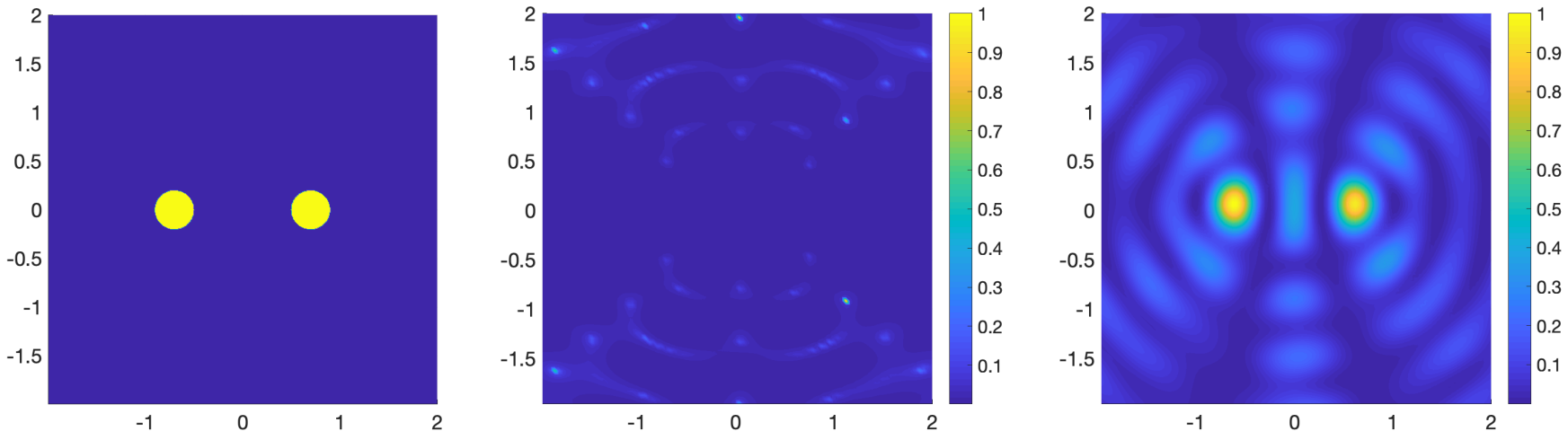

(e) True geometry **(f)** LSM, no noise **(g)** $I(z)$, 30% noise

Figure: Reconstruction with one-wave data using the classical linear sampling method (LSM) and the sampling method with $I(z)$ ($k = 6$).

Numerical simulations

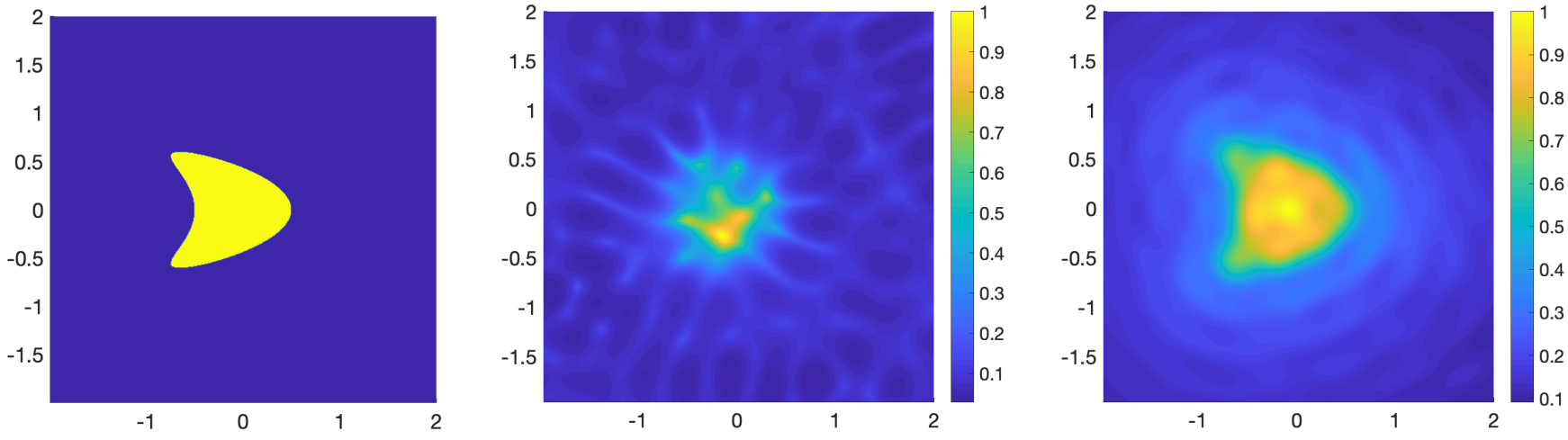

(a) True geometry **(b)** LSM, 30% noise **(c)** $I(z)$, 30% noise

Figure: Reconstruction with multi-wave data using the classical linear sampling method (LSM) and the sampling method with $I(z)$ (64 incident waves, $k = 8$).

Numerical simulations

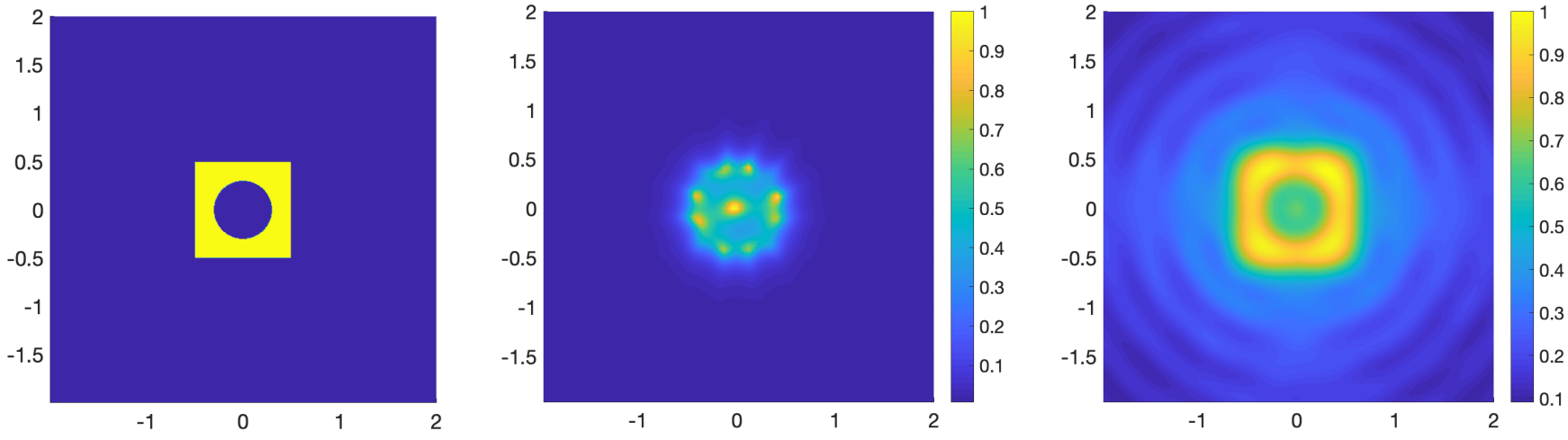

(a) True geometry **(b)** LSM, 3% noise **(c)** $I(z)$, 30% noise

Figure: Reconstruction with multi-wave data using the classical linear sampling method (LSM) and the sampling method with $I(z)$ (96 incident waves, $k = 8$).

Experimental data verification (joint with T. Le and T. Truong)

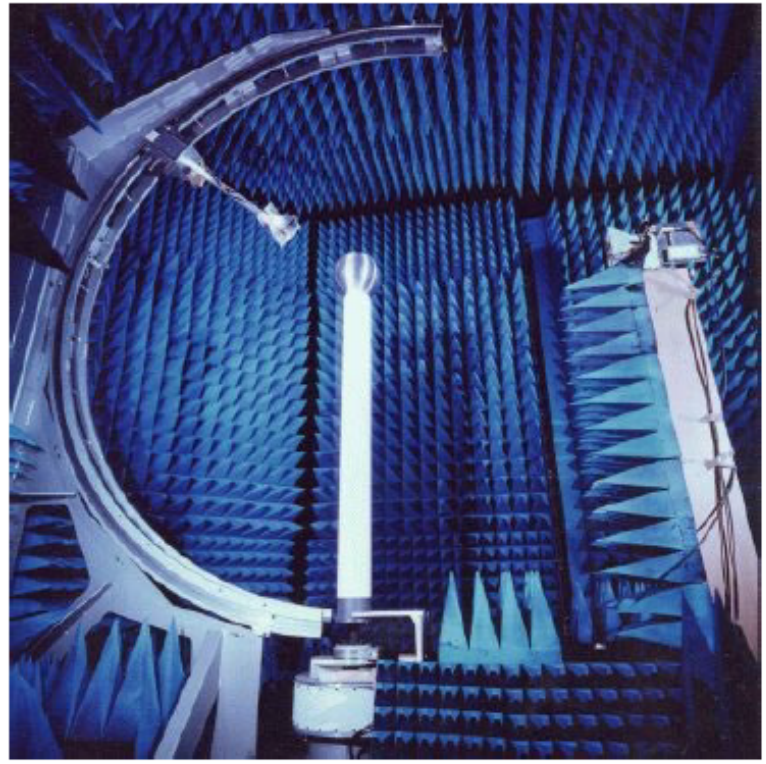

Figure: The data are measured in the anechoic chamber at the Centre Commun de Ressources Micro-ondes (CCRM) of the Fresnel Institute at Marseille.

Experimental data verification (joint with T. Le and T. Truong)

Recall the Sommerfield radiation condition

$$\lim_{|x|\to\infty} |x| \left(\frac{x}{|x|} \cdot \nabla u^{sc} - iku^{sc} \right) = 0,$$

and

$$I(z) = \int_S \left| \int_{\partial\Omega} \left(\frac{\partial \mathrm{Im}\, \Phi(x,z)}{\partial \nu(x)} u^{sc}(x,\theta) - \mathrm{Im}\, \Phi(x,z) \frac{\partial u^{sc}(x,\theta)}{\partial \nu(x)} \right) ds(x) \right|^2 ds(\theta).$$

Define

$$I_{far}(z) := \int_S \left| \int_{\partial\Omega} \left(\frac{\partial \mathrm{Im}\, \Phi(x,z)}{\partial \nu(x)} u^{sc}(x,\theta) - ik \mathrm{Im}\, \Phi(x,z) u^{sc}(x,\theta) \right) ds(x) \right|^2 ds(\theta).$$

If $\partial\Omega = \{x \in \mathbb{R}^2 : |x| = R\}$, then

$$I_{far}(z) = I(z) + O\left(\frac{1}{R}\right), \quad R \to \infty$$

Experimental data verification (joint with T. Le and T. Truong)

Scaling: 40 mm $\sim$ 1. Frequency = 8 GHz ($k \approx 6.7$). Target: dielectric disk of radius 15 mm (~ 0.375). The distance from the disk's center to the origin is 30 mm (~ 0.75). Measurement distance from the origin is 0.76 m (~ 19). Multi-wave data matrix size: 72 (receivers) $\times$ 36 (incident sources).

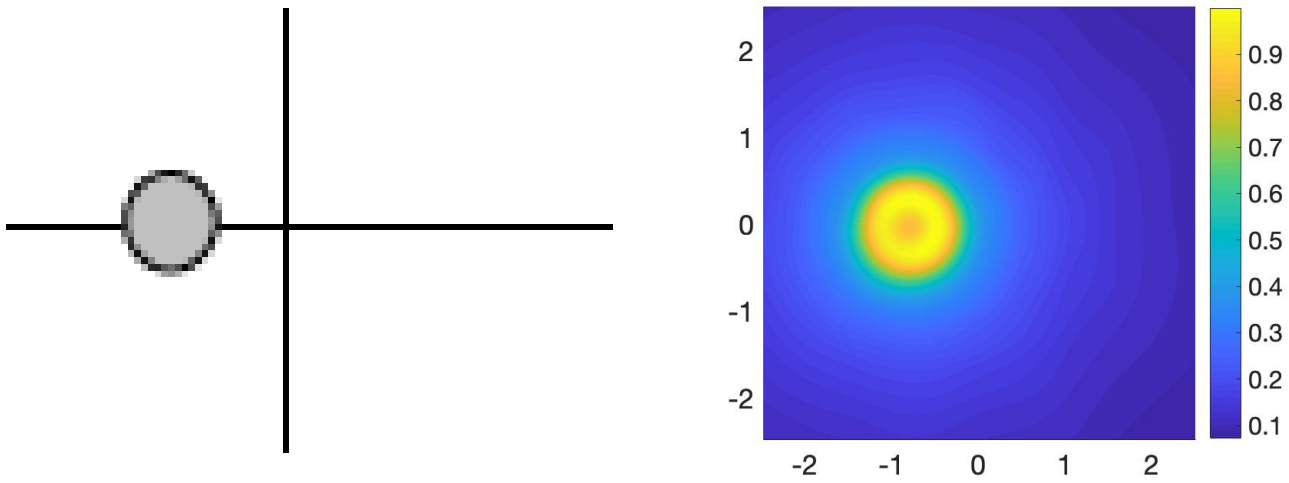

(a) True geometry **(b)** Reconstruction

Figure: Reconstruction with experimental data using $I_{far}(z)$.

Experimental data verification (joint with T. Le and T. Truong)

Scaling: 40 mm $\sim$ 1. Frequency = 12 GHz ($k \approx 10$). Target: metallic U-shaped object of size 50 mm $\times$ 80 mm ($\sim 1.25 \times 2$). Measurement distance from the origin is 0.76 m (~ 19). Multi-wave data matrix size: 72 (receivers) $\times$ 36 (incident sources).

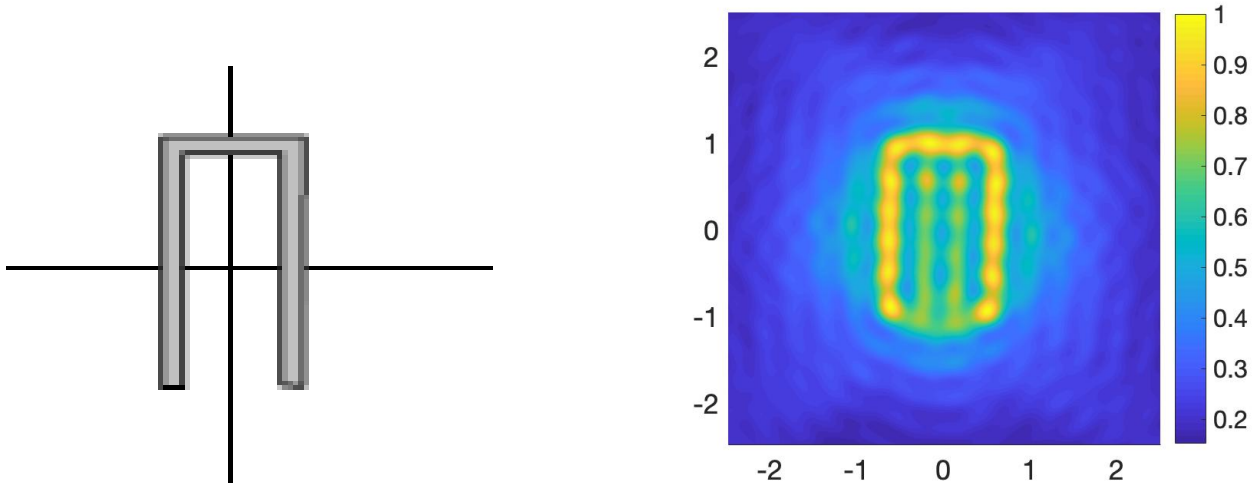

(a) True geometry **(b)** Reconstruction

Figure: Reconstruction with experimental data using $I_{far}(z)$.

Outline

1. Introduction
   - Inverse scattering: motivations and challenges
   - Why global reconstruction methods?
2. An inverse medium scattering problem
   - Sampling method
   - Numerical study for simulated and experimental data
3. Locating and quantifying point scatterers
   - Sampling method
   - Numerical simulations

Locating and quantifying point scatterers

- Consider the scattering of incident wave $u^{\text{in}}(x) = e^{ikx\cdot\theta}$ by M point scatterers located at $x_1, \ldots, x_M$ in $\mathbb{R}^2$. Let $\alpha_j \in \mathbb{C}$ be scattering strength of the j-th scatterer.

- If multiple scattering between scatterers are neglected, scattered wave u^{sc} is given by

$$u^{\text{sc}}(x) = \sum_{j=1}^{M} \alpha_j \, \Phi(x, x_j) \, u^{\text{in}}(x_j),$$

  where Φ is the Green's function.

- **Inverse Problem.** Determine locations x_j and scattering strengths α_j, $j = 1, \ldots, M$, of the point scatterers from one-wave Cauchy data of the scattered field u_{sc}.

Locating and quantifying point scatterers

- Imaging point-like scatterers has been studied mostly by MUSIC-type algorithms (MUSIC stands for MUltiple SIgnal Classification)
- For instance: Cheney 2001, Kirsch 2002, Devaney 2005, Ammari et al 2006, Martin 2006, Challa et al 2012, Fazli et al 2012, Griesmaier et al 2017, Chen 2018.
- Most these works are concerned with locating point-like scatterers. To compute the scattering strengths, one typically has to solve a least-square problem using some iterative method.
- The sampling method we study can be extended to image point scatterers in a simple way.

Locating and quantifying point scatterers

Define

$$\widetilde{I}(z) := \int_{\partial\Omega} \left(\frac{\partial \mathrm{Im}\, \Phi(x,z)}{\partial \nu(x)} u^{sc}(x) - \mathrm{Im}\, \Phi(x,z) \frac{\partial u^{sc}(x)}{\partial \nu(x)} \right) ds(x).$$

Lemma.

$$\widetilde{I}(z) = \sum_{j=1}^{M} \alpha_j J_0(k|z - x_j|) e^{ikx\cdot\theta}.$$

Assume that

$$L := \min_{1\le i,j\le M, i\neq j} \mathrm{dist}(x_i, x_j) \gg \frac{2\pi}{k}.$$

Then the locations x_j can be determined by the peaks of $|\widetilde{I}(z)|$. After $\{x_j\}_{j=1,\ldots,M}$ are obtained, scattering strengths α_j can be approximately computed by

$$\alpha_j = e^{-ikx_j\cdot\theta} \widetilde{I}(x_j) + O\left(\frac{1}{\sqrt{kL}}\right), \quad j = 1, \ldots, M.$$

Numerical simulations

- Target: One point scatterer located at $(0.5, 0.5)$ with scattering strength $\alpha = 1 + 2i$.
- Reconstruction: location $= (0.5, 0.5)$, scattering strength $= 0.9369 + 2.0120i$.

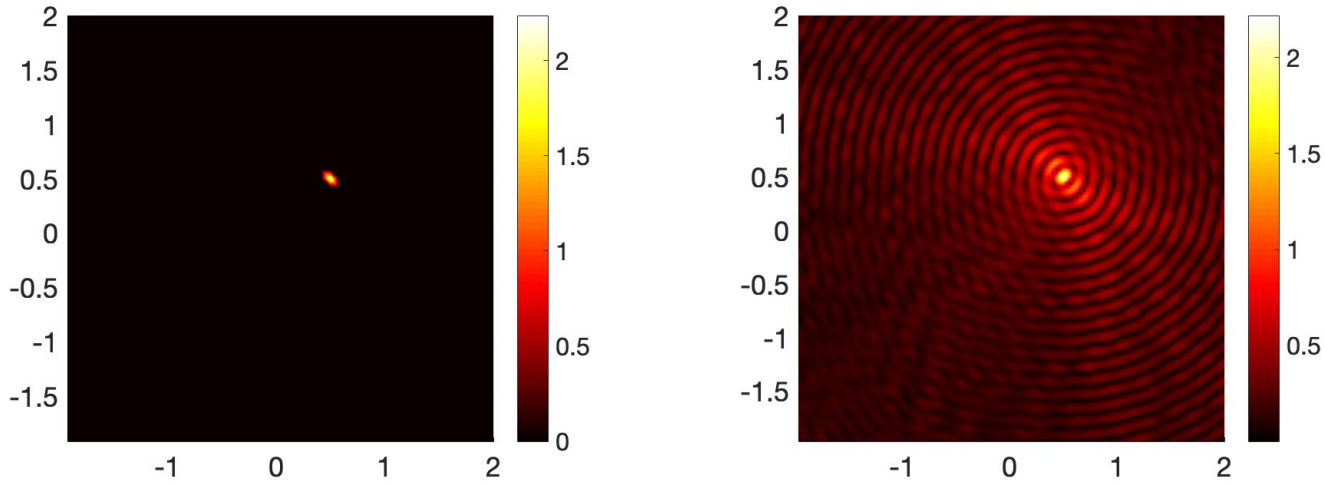

(a) True geometry **(b)** Reconstruction

Figure: Imaging one point scatterer with $u^{in} = e^{ik(x_1 \cos\varphi x_1 + x_2 \sin\varphi)}$, $k = 25, \varphi = \pi/4$, 30% noise in data.

Numerical simulations

- Target: Two point scatterers located at $(-0.5, 0.5)$ with $\alpha_1 = 1 - 2i$ and at $(1, -1)$ with $\alpha_2 = 1 + 2i$.
- Reconstruction: location $= (-0.5, 0.5)$, $\alpha_1 = 0.9203 - 2.0285i$, location $= (1, -1)$, $\alpha_2 = 0.9499 + 2.0899i$.

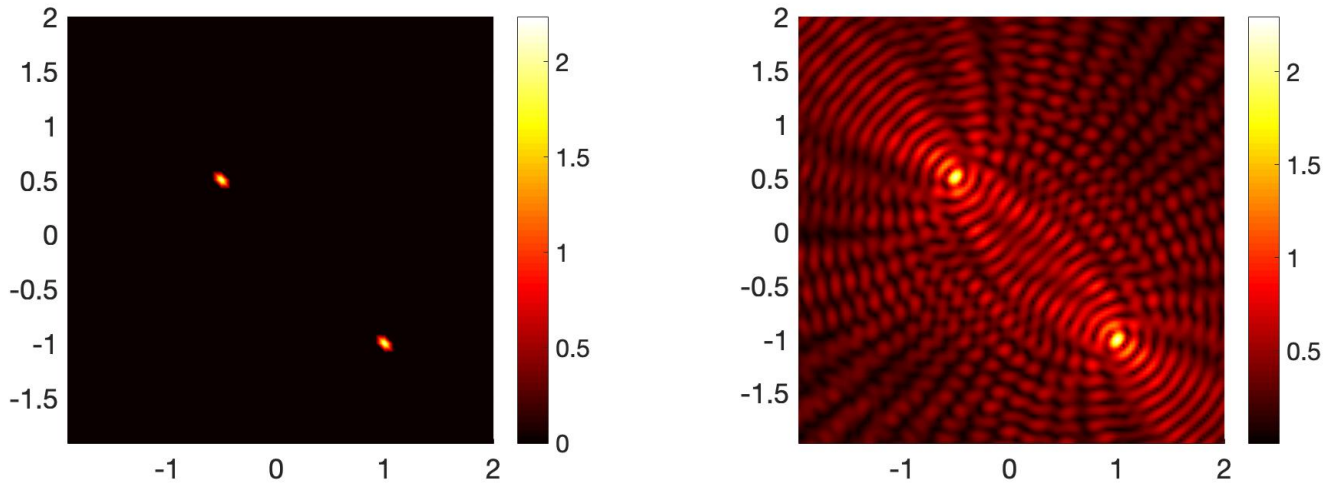

(a) True geometry **(b)** Reconstruction

Figure: Imaging two point scatterers with $u^{in}(x) = e^{ik(x_1 \cos\varphi x_1 + x_2 \sin\varphi)}$, $k = 25, \varphi = \pi/4$, 30% noise in data.

Conclusion

We propose a sampling method of orthogonality sampling type for inverse scattering problems.

- Simple and fast implementation
- Stable against noise in the data
- Versatile: applicable to various types of data such as near-field/far-field data, one-wave/multi-wave/multi-frequency data
- Verified by experimental data from the Fresnel Institute
- Applicable to quantitative imaging of point-scatterers

Thank you for listening!